Supplemental Figures

Figure S1, related to Figure 1

A

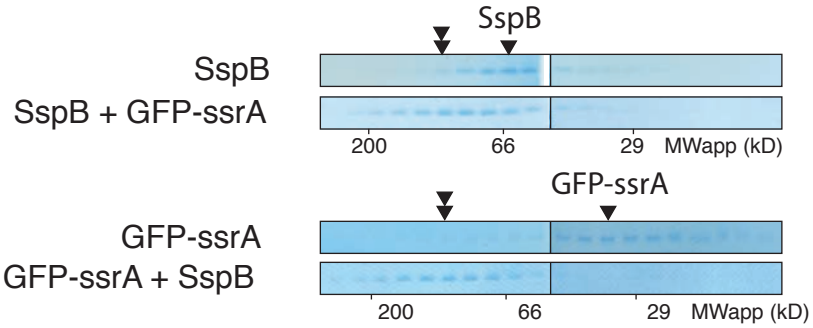

B Coomassie staining

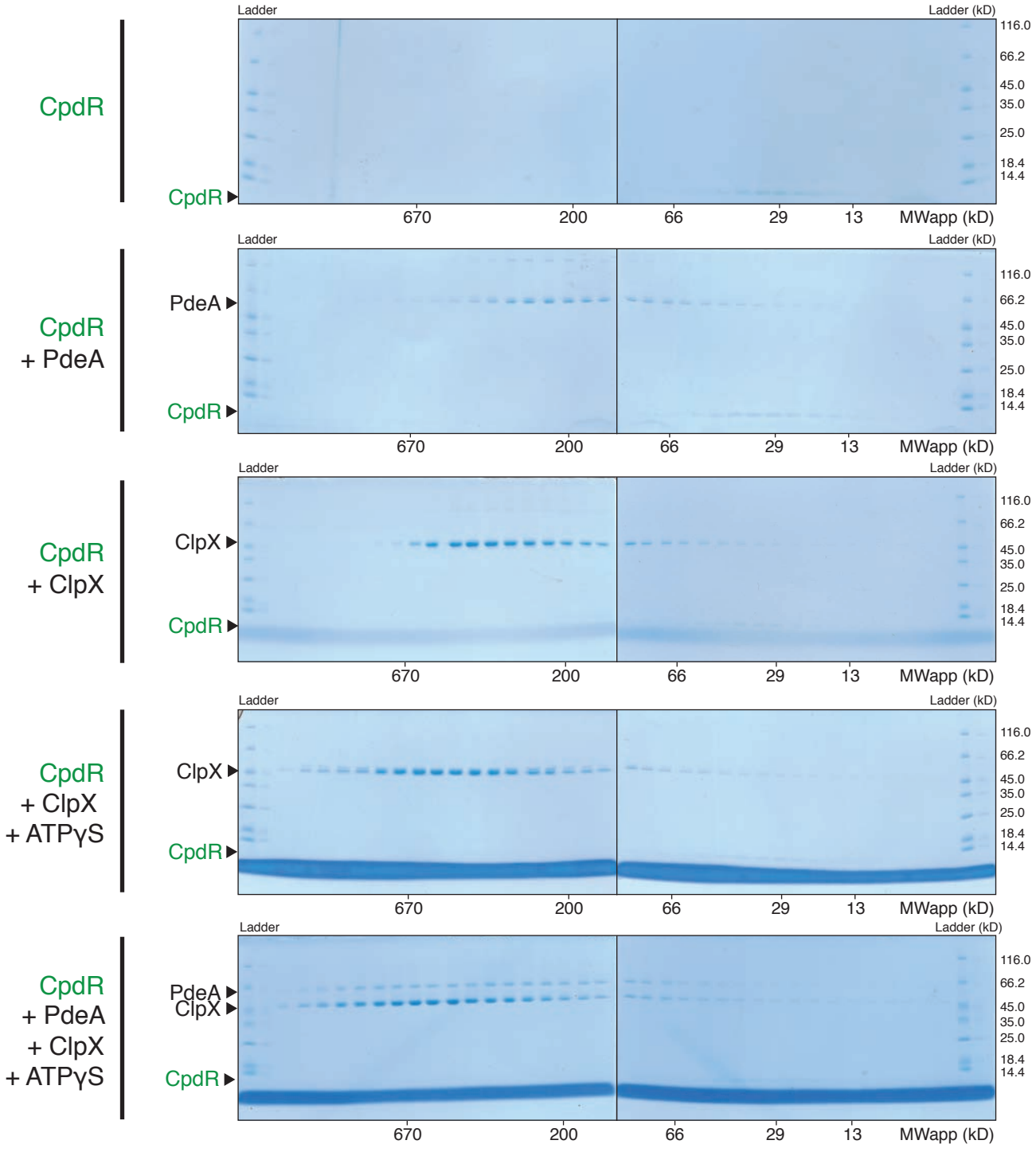

Figure S1 B continued

Silver staining

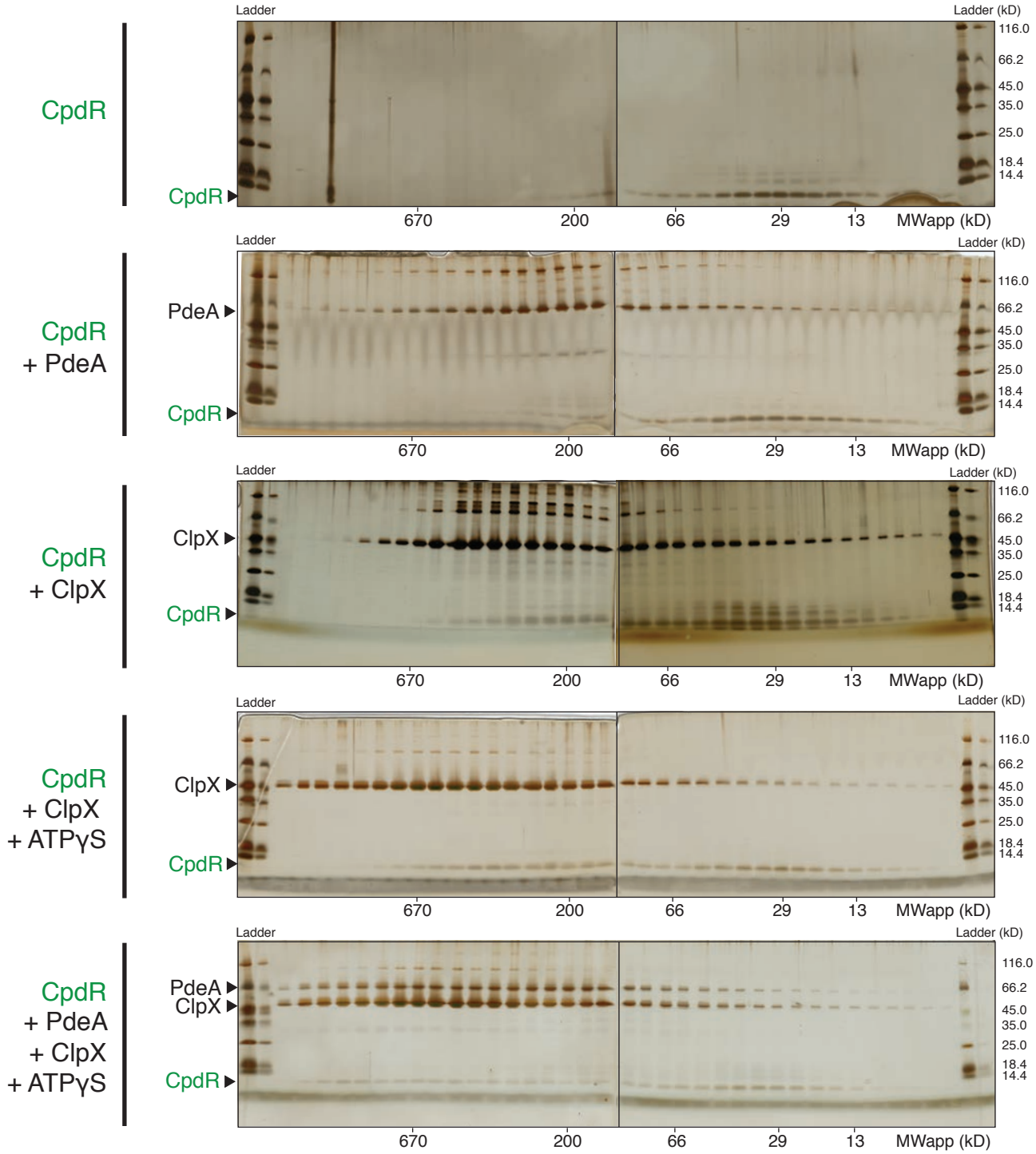

Figure S1

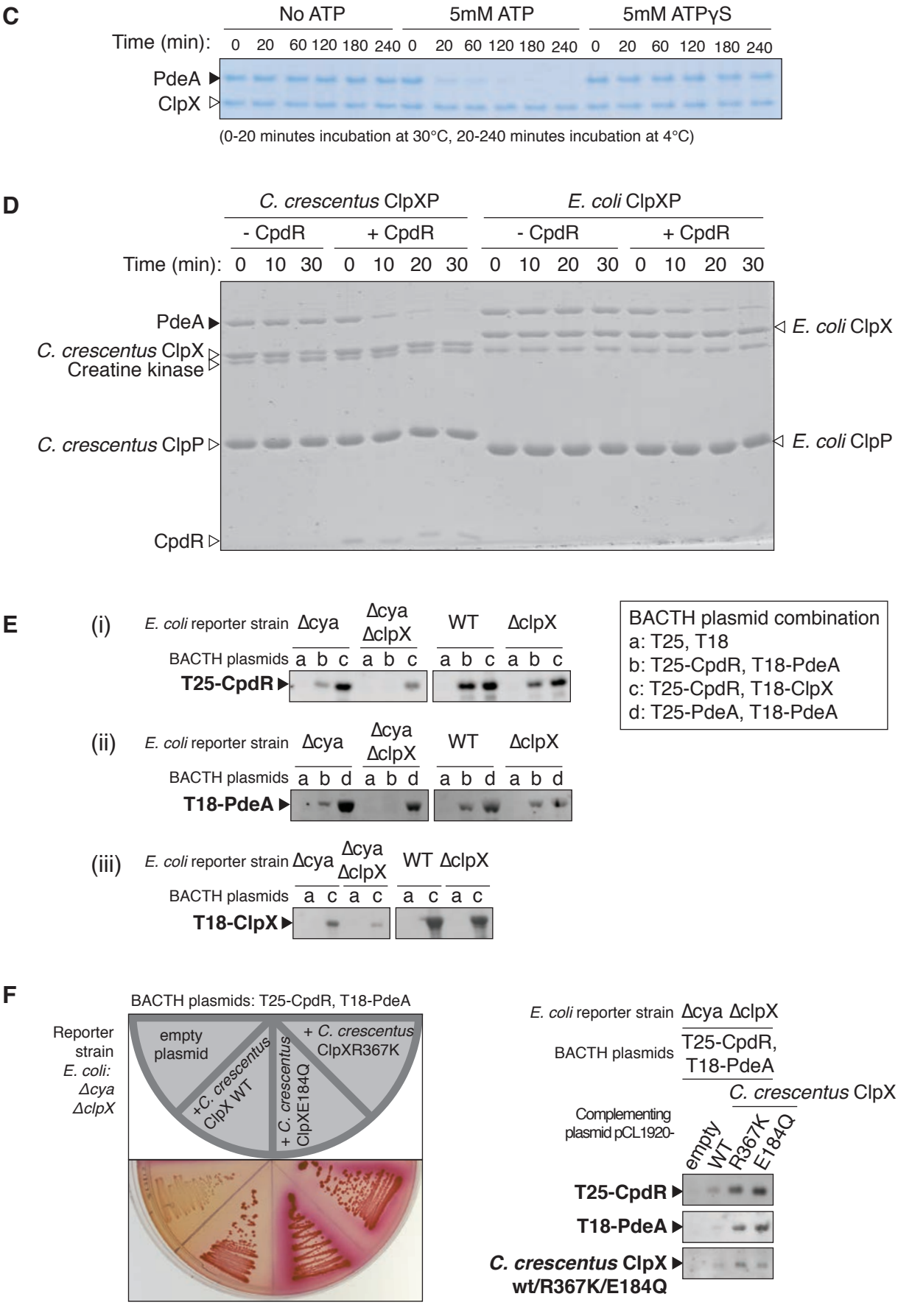
C
No ATP
5mM ATP
5mM ATPγS
Time (min): 0 20 60 120 180 240 0 20 60 120 180 240 0 20 60 120 180 240
PdeA
ClpX
(0-20 minutes incubation at 30°C, 20-240 minutes incubation at 4°C)
D
C. crescentus ClpXP
E. coli ClpXP
- CpdR
+ CpdR
Time (min): 0 10 30 0 10 20 30 0 10 20 30 0 10 20 30
PdeA
C. crescentus ClpX
Creatine kinase
C. crescentus ClpP
CpdR
E. coli ClpX
E. coli ClpP
E
(i)
E. coli reporter strain Δcya Δcya ΔclpX WT ΔclpX
BACTH plasmids a b c a b c a b c a b c
T25-CpdR
(ii)
E. coli reporter strain Δcya Δcya ΔclpX WT ΔclpX
BACTH plasmids a b d a b d a b d a b d
T18-PdeA
(iii)
E. coli reporter strain Δcya Δcya ΔclpX WT ΔclpX
BACTH plasmids a c a c a c a c
T18-ClpX
BACTH plasmid combination
a: T25, T18
b: T25-CpdR, T18-PdeA
c: T25-CpdR, T18-ClpX
d: T25-PdeA, T18-PdeA
F
BACTH plasmids: T25-CpdR, T18-PdeA
Reporter strain E. coli: Δcya ΔclpX
empty plasmid
+C. crescentus ClpX WT
+ C. crescentus ClpXE184Q
+ C. crescentus ClpXR367K
E. coli reporter strain Δcya ΔclpX
BACTH plasmids T25-CpdR, T18-PdeA
C. crescentus ClpX
Complementing plasmid pCL1920-
empty
WT
R367K
E184Q
T25-CpdR
T18-PdeA
C. crescentus ClpX wt/R367K/E184Q

Figure S2, related to Figure 2 and Figure 6

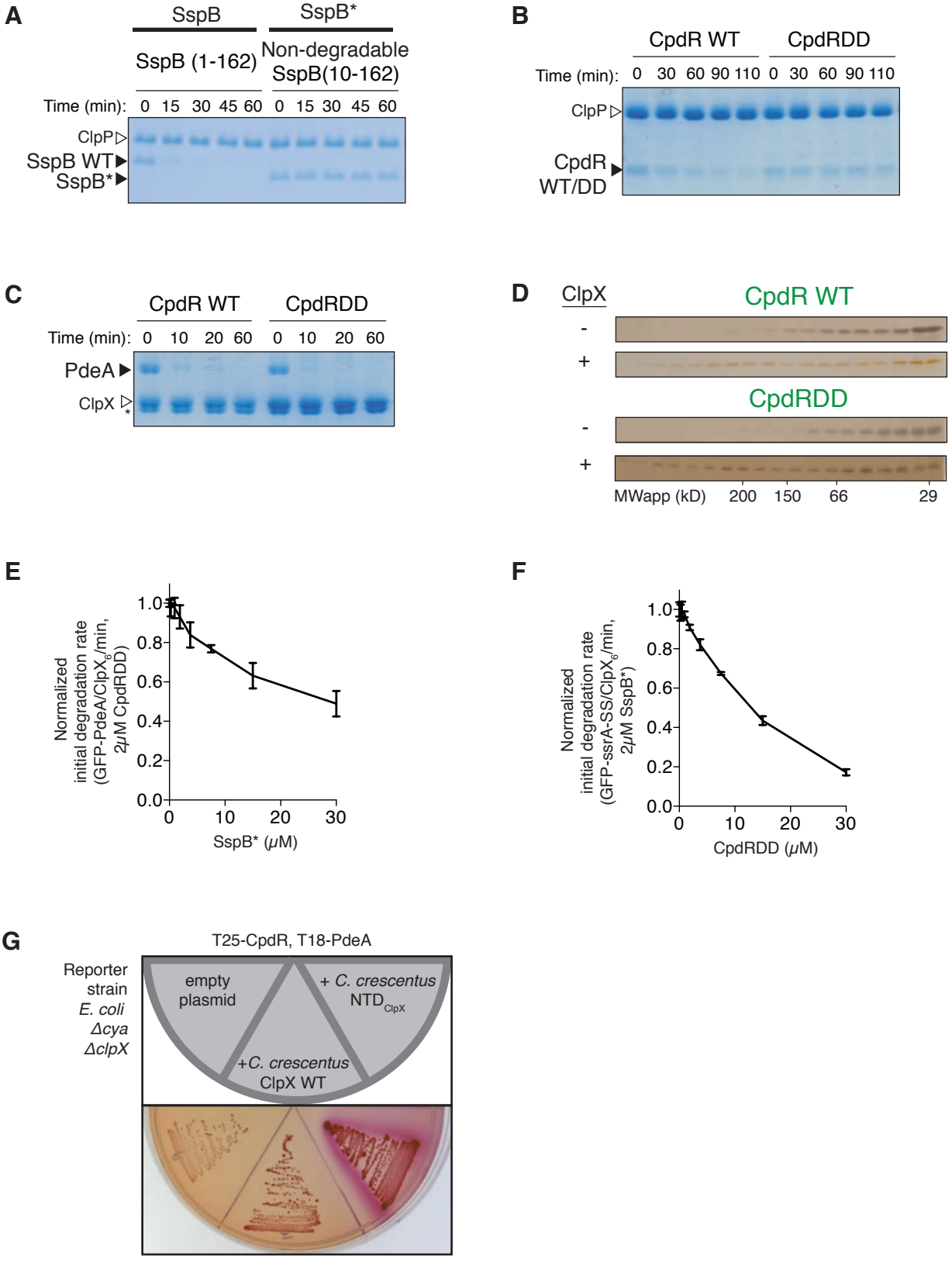

Figure S3, related to Figure 3

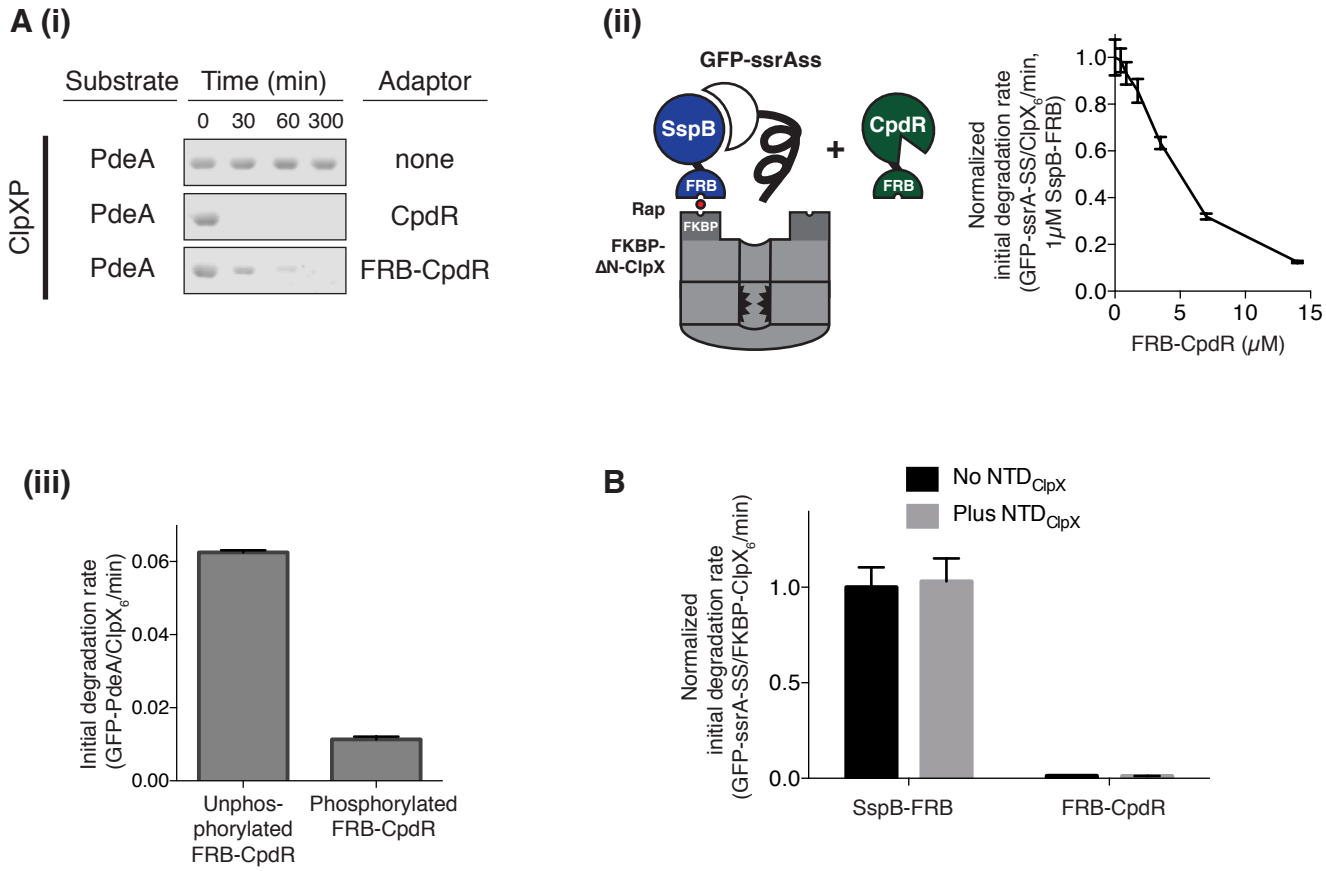

Figure S4, related to Figure 4

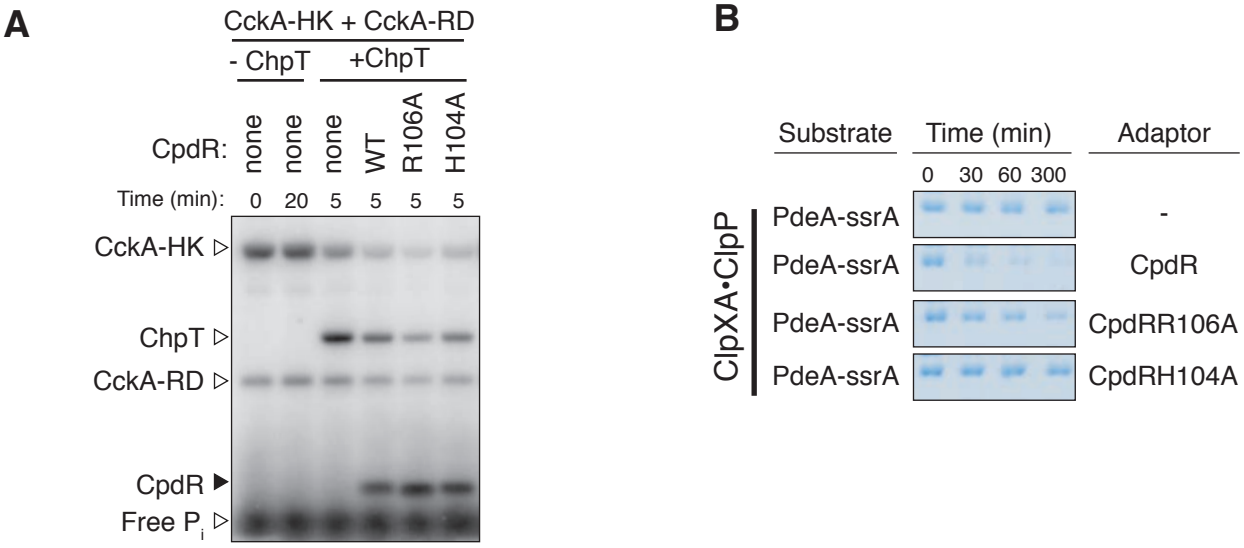

Figure S5, related Figure 5

A *C. crescentus* Δ*cpdR*
pRX-M2-CpdR variants

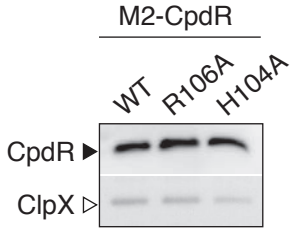

B *C. crescentus* wildtype
pHX-M2-CpdR variants

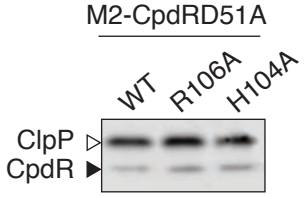

C *C. crescentus* Δ*pdeA*
pHX-M2-CpdR variants

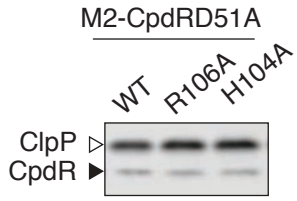

D *C. crescentus* Δ*cpdR clpX-gfp*
pHX-M2-CpdR variants

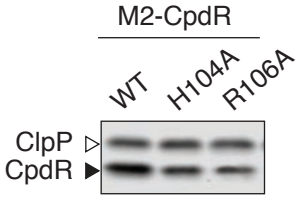

E *C. crescentus* Δ*cpdR*
pHX-M2-CpdR variants

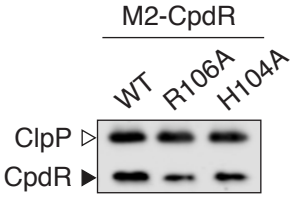

Figure S6, related to Figure 6

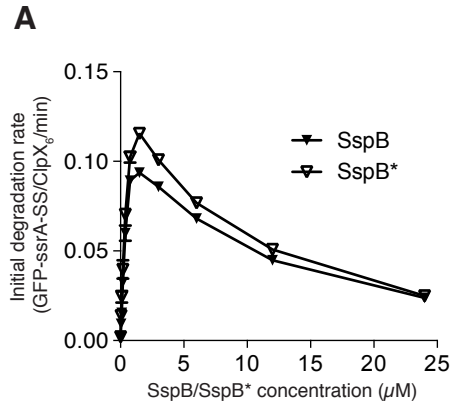

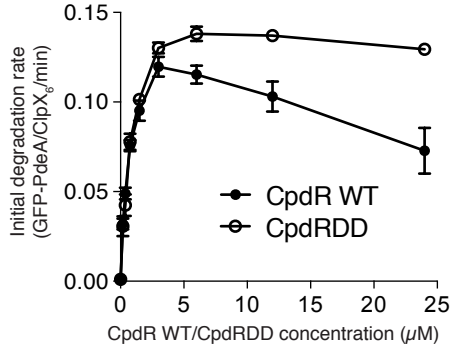

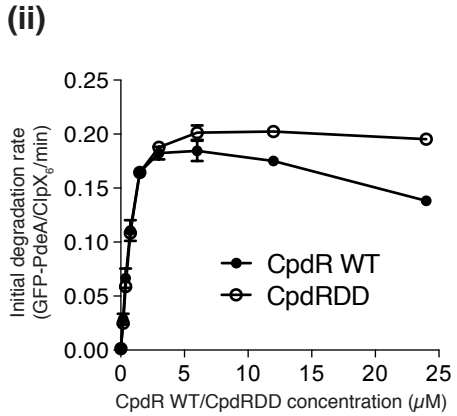

Figure S6

C

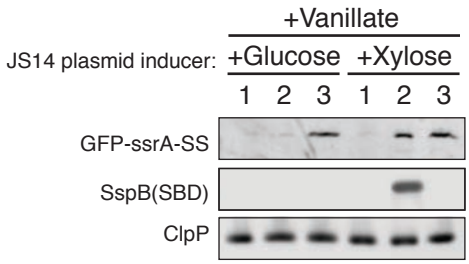

Strain description
1: *C. crescentus* P_{van}-GFP-ssrA-SS, empty plasmid JS14
2: *C. crescentus* P_{van}-GFP-ssrA-SS, plasmid JS14 P_{xyl}-SspB (substrate binding domain)
3: *C. crescentus* P_{van}-GFP-ssrA-SS Δ*sspB*, empty plasmid JS14

D (i)

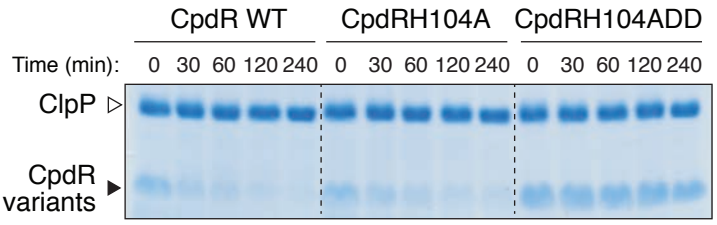

(ii)

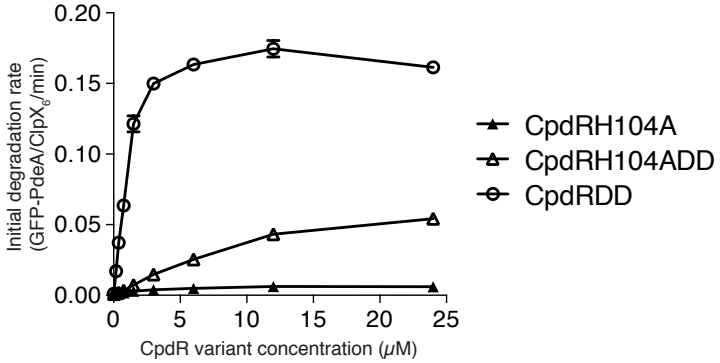

E

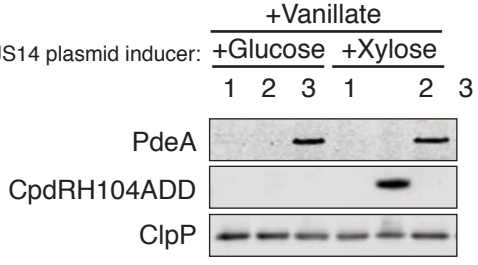

Strain description
1: *C. crescentus* P_{van}-PdeA, empty plasmid JS14
2: *C. crescentus* P_{van}-PdeA, plasmid JS14 P_{xyl}-CpdRH104ADD
3: *C. crescentus* P_{van}-PdeA Δ*cpdR*, empty plasmid JS14

Figure S7, related to Figure 7

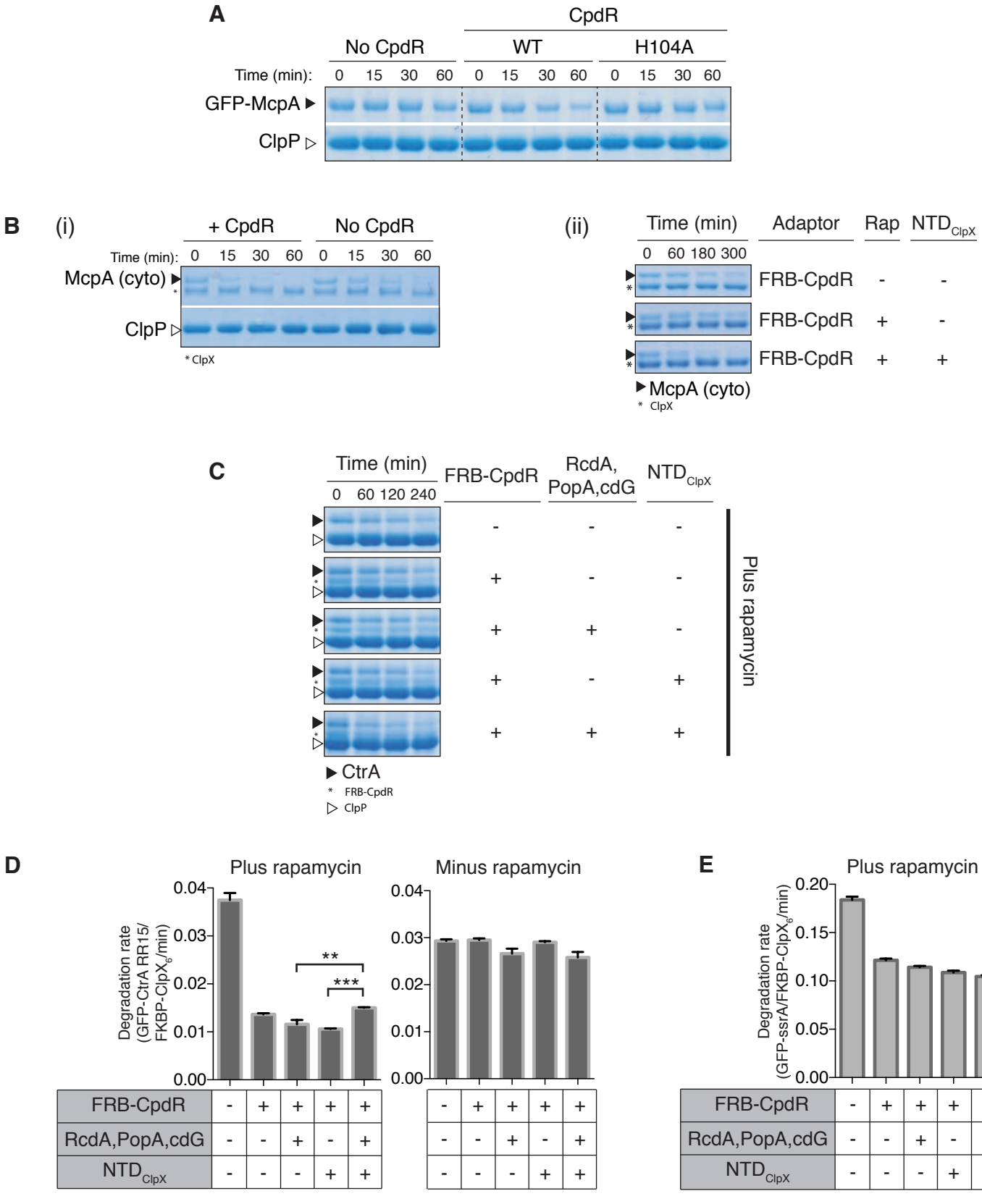

SUPPLEMENTAL FIGURE LEGENDS

Figure S1, related to Figure 1.

(A) Interaction between SspB and GFP-ssrA by size exclusion chromatography (SEC). SEC interaction profiles of the *C. crescentus* protein orthologs of GFP-ssrA (5μM) and SspB (10μM). Single triangles: peaks of the proteins (based on 280 nm) by themselves; double triangles: peaks of the proteins (based on 280 nm) when the adaptor and substrate are mixed.

(B) Full-size gels of SEC profiles of CpdR, PdeA, and ClpX (cropped versions of these are shown in Figure 1B). SEC profiles of CpdR (±PdeA/ClpX/ATPγS), as shown in Figure 1B, examined by Coomassie staining followed by silver staining are shown in full size. 36 fractions from the SEC were analyzed across two separate twenty-well SDS-PAGE gels. Gels were stained with Coomassie stain prior to silver stain. Molecular weight ladder was loaded in equivalent amounts in two lanes per gel (Thermo Scientific unstained protein molecular weight marker 1/10 dilution in one well, and 1/50 dilution in the well after). In these SEC experiments, 20μM CpdR/5μM PdeA/5μM $ClpX_6$/5mM(sample mixture) or 1mM (in running buffer) ATPγS were used, with 1mM GTP throughout.

(C) ATPγS cannot support CpdR-mediated ClpXP degradation of PdeA. Degradation profile of PdeA (1μM) by ClpXP (0.4μM $ClpX_6$, 0.8μM $ClpP_{14}$) mediated by CpdR (2μM) in the presence of ATP or the slowly hydrolyzed ATP analog, ATPγS (5mM). 1mM GTP is present in the reactions. Temperature of incubation reflects the procedure used for analytical size exclusion chromatography studies in this work, where samples are incubated 25°C for 20 minutes in the presence of 5mM ATPγS before injection onto the column at 4°C for 30 minutes elution time (the running buffer contained 1mM ATPγS).

(D) CpdR-dependent degradation of PdeA by *E. coli* ClpXP. *In vitro* degradation of PdeA (1μM) by *C. crescentus* and *E. coli* orthologs of ClpXP (0.3μM $ClpX_6$, 0.5μM $ClpP_{14}$) when mediated by CpdR (2μM) in the presence of ATP and a regeneration system, and 1mM GTP. Samples were examined by Coomassie staining of SDS-PAGE gel (shown here as greyscale).

(E) Bacterial adenylate cyclase two hybrid (BACTH) plasmid expression level evaluated by Western blot. Protein expression of BACTH plasmids (Figure 1D) in the *E. coli* reporter strains BTH101 (Δ*cya*) and BTH101 Δ*clpX (*Δ*cya* Δ*clpX)* were measured after cells were plated and incubated on McConkey agar containing 1% maltose, 1mM IPTG, 100μg/mL ampicillin, 50μg/mL kanamycin. Because bait/prey are induced from lac promoters, expression levels will reflect the strength of adenylate cyclase complementation in Δ*cya* strains. To control for this, expression of bait/prey was also measured in wildtype W3110 strain (WT) strains and W3110 strains lacking endogenous ClpX *(*Δ*clpX*), where cells were harvested after growth in LB containing 1mM IPTG, 100μg/mL ampicillin, 50μg/mL kanamycin. Cell density (OD600) measurements were used to normalize the amounts of cells harvested for each sample.
(i) T25-CpdR protein levels in the presence of plasmids expressing T18-PdeA or T18-ClpX, detected by Western using α- CpdR.
(ii) T18-PdeA protein levels in the presence of plasmids expressing T25-CpdR or T25-PdeA, detected by Western using α-PdeA.

(iii) T18-ClpX protein level in the presence of plasmid expressing T25-CpdR, detected by Western using α-*C. crescentus* ClpX.

(F) Complementation of the BACTH reporter strain, *E. coli* Δ*cya* Δ*clpX, by C. crescentus clpX ortholog* and its ATPase variants *clpX*E184Q and *clpX*R367K. *E. coli BTH101* Δ*clpX* (Δ*cya* Δ*clpX*) strains that contained three compatible plasmids (1) pKT25-CpdR, (2) pUT18C-PdeA, and (3) pCL1920 empty plasmid or pCL1920 expressing *C. crescentus* ClpX WT or ClpX E184Q or R367K, were generated. Sequence alignments with *E. coli* ClpX indicate that *C. crescentus* ClpX E184Q is the ATPase mutant equivalent of *E. coli* ClpX E185Q, which does not hydrolyze ATP, but promotes a ClpX conformation that binds ClpP or ssrA-tagged substrates (Hersch et al., 2005), while *C. crescentus* ClpX R367K is the ATPase mutant equivalent of *E. coli* ClpX R370K, which is mutated in the sensor-2 motif, preventing ATP hydrolysis, and is locked in an inactive ClpX conformation unable to bind ClpP or ssrA-tagged substrates (Joshi et al., 2004). Colonies were restreaked on McConkey agar containing 1% maltose, 1mM IPTG, 100μg/mL ampicillin, 50μg/mL kanamycin, and 50μg/mL spectinomycin.

Positive BACTH interaction between CpdR and PdeA in the presence of ClpX WT, E184Q and R367K indicates that the ternary interaction between CpdR, PdeA and ClpX is not reliant on ClpX ATP hydrolysis and the (active or inactive) conformation of the ATPase domain of ClpX.

T25-CpdR, T18-PdeA and *C. crescentus* ClpX WT/E184Q/R367K protein expression in the cell were detected by Western using α-CpdR, α-PdeA and α-*C. crescentus* ClpX (cells were harvested after plating on McConkey agar containing 1% maltose, 1mM IPTG, 100μg/mL ampicillin, 50μg/mL kanamycin, and 50μg/mL spectinomycin).

(A-B) performed in duplicates. (E&F) performed in triplicates. Representative gels are shown.

Figure S2, related to Figure 2 and Figure 6.

(A) *In vitro* degradation of SspB* (residues 11-162) versus wildtype SspB (1-162) by ClpXP. *C. crescentus* SspB (1-162) is degradable unless its N-terminus ten amino acid is removed to reveal an alternative methionine start site which produces a stable, but completely active form of SspB (Chien et al., 2007a). Degradation of full length SspB (residues 1-162) and stable SspB* (residues 11-162) (4μM) by ClpXP (0.2μM $ClpX_6$, 0.4μM $ClpP_{14}$) are shown for comparison.

(B) *In vitro* degradation of CpdR wildtype (WT) and its non-degradable variant CpdRDD (C-terminal Ala-Ala mutated to Asp-Asp) by ClpXP. CpdR WT and CpdRDD (10μM) degradation by ClpXP (0.2μM $ClpX_6$, 0.4μM $ClpP_{14}$) are shown for comparison.

(C) The non-degradable variant CpdRDD mediates ClpXP degradation of PdeA *in vitro*. The adaptor function of CpdR WT and CpdRDD (2μM) evaluated by comparing their activity in mediating degradation of PdeA (1μM, in the presence of 1mM GTP) by ClpXP (0.4μM $ClpX_6$, 0.8μM $ClpP_{14}$).

(D) The non-degradable variant CpdRDD interacts with ClpX. Size exclusion chromatography profiles of 20μM CpdR WT/DD in the presence of 5μM $ClpX_6$. Protein profiles were determined by silver staining.

(E) SspB competes with CpdR-dependent degradation *in vitro*. 0-30μM SspB* was added to the degradation reaction of GFP-PdeA (1μM) by ClpXP (0.2μM $ClpX_6$, 0.4μM $ClpP_{14}$) with CpdRDD (2μM). 1mM GTP is present in the reactions.

(F) CpdR competition with SspB-dependent degradation *in vitro*. 0-30μM CpdRDD was added to the degradation reaction of GFP-ssrA (1μM) by ClpXP (0.2μM $ClpX_6$, 0.4μM $ClpP_{14}$) with SspB* (2μM).

The non-degradable versions of CpdR (CpdRDD) and SspB (residues 11-162, SspB*) are used in (E,F) to avoid complications that could occur due to trivial competition of the degradation of the adaptors with the degradation of their cognate substrates.

(G) Complementation of the BACTH reporter strain, *E. coli* Δ*cya* Δ*clpX*, by NTD_{ClpX}. *E. coli BTH101* Δ*clpX* (Δ*cya* Δ*clpX*) strains that contained three compatible plasmids: (1) pKT25-CpdR, (2) pUT18C-PdeA, and (3) pCL1920 empty plasmid or pCL1920 expressing *C. crescentus* ClpX WT or NTD_{ClpX}, were generated. Colonies were restreaked on McConkey agar containing 1% maltose, 1mM IPTG, 100μg/mL ampicillin, 50μg/mL kanamycin, and 50μg/mL spectinomycin.

(A, B, & D) performed in duplicates. (C, E, F & G) performed in triplicates.

Figure S3, related to Figure 3.

(A) Characteristics of the FRB-CpdR protein. (i) *In vitro* degradation of PdeA (1μM) by ClpXP (0.4μM $ClpX_6$, 0.8μM $ClpP_{14}$) mediated by CpdR/FRB-CpdR (2μM). The results indicate that FRB-CpdR is less active than CpdR WT but retains adaptor functionality. (ii) Assay to check whether FRB-CpdR competes with SspB-FRB-mediated delivery, indicating FRB-CpdR binds FKBP-ΔN-ClpX in the presence of rapamycin. Cartoon shows SspB-FRB-dependent delivery of GFP-ssrA-SS to FKBP-ΔN-ClpXP in the presence of rapamycin. FRB-CpdR was added to see if it could compete with SspB-FRB for binding to FKBP-ΔN-ClpX. Initial rates of degradation of GFP-ssrA-SS (1.5μM) mediated by 1μM SspB-FRB/0.4μM FKBP-ΔN-$ClpX_6$/0.8μM $ClpP_{14}$/10μM rapamycin in the presence of increasing concentrations of FRB-appended CpdRs are shown on the right. Together with the rescue of degradation shown in Figure 3C, this shows that the FRB portion of FRB-CpdR can bind FKBP. Data are represented as mean ± SD, n = 3 experiments. (iii) *In vitro* degradation of GFP-PdeA (1μM) by ClpXP mediated by 3μM FRB-CpdR or phosphorylated FRB-CpdR. Phosphorylation was performed using the CpdR cognate phosphorelay CckA/ChpT (Biondi et al., 2006; Chen et al., 2009) by preincubation with 1.5μM CckA-HK, 0.75μM CckA-RD, 0.5μM ChpT, and 5mM ATP for 40 minutes. Data are represented as mean ± SD, n = 3 experiments. The results indicate that, like wildtype CpdR, the FRB-CpdR ability to mediate substrate delivery to ClpXP can be inactivated by phosphorylation.

(B) Effect of NTD_{ClpX} on delivery of GFP-ssrA-SS by adaptors SspB-FRB/FRB-CpdR when tethered to FKBP-ΔN-ClpXP. As a control for experiments shown in Figure 3C and D, we monitored delivery of 1μM substrate GFP-ssrA-SS to 0.4μM FKBP-ΔN-$ClpX_6$/0.8μM $ClpP_{14}$/10μM rapamycin with 3μM SspB-FRB/FRB-CpdR in the absence and presence of 25μM NTD_{ClpX} fragment.

(A,B) performed in triplicates. Representative gels are shown in A.

Figure S4, related to Figure 4.

(A) CpdR wildtype and variants, R106A and H104A, are phosphorylatable. *In vitro* phosphorelay profiling of CpdR wildtype (WT), and variants R106A and H104A using radiolabeled ATP (^{32}P). A split version of CckA in which the histidine kinase (CckA-HK) and receiver domains (CckA-RD) are separate polypeptides were used to minimize dephosphorylation (Chen et al., 2009). ChpT is a phosphotransferase that mediates phosphotransfer from CckA to CpdR (Biondi et al., 2006). See Supplementary Experimental Procedures for details on the radioactive phosphotransfer method.

(B) CpdR variants R106A and H104A show ranked order activity compared to wildtype CpdR in mediating degradation by ClpXAP. *In vitro* degradation of 1μM PdeA-ssrA by the chimeric ClpXAP (0.4μM $ClpXA_6$, 0.8μM $ClpP_{14}$) when mediated by CpdR WT/ R106A/H104A variants (2μM).

(A,B) performed in triplicates. Representative gels are shown.

Figure S5, related to Figure 5.

***In vivo* expression levels of Flag M2-tagged CpdR variants in *C. crescentus* strains evaluated in Figure 5 and 7.** *C. crescentus* strains expressing CpdR variants were grown at 30°C in a shaking incubator in PYE containing the relevant antibiotics overnight before dilution into fresh antibiotic-containing media supplemented with 0.2% xylose for 6 hours induction. Cells were harvested at exponential phase (OD600<1). Cell density (OD600) measurements were used to normalize the amounts of cells harvested for each sample. Flag-M2-tagged CpdR were detected by Western using α-Flag (filled triangles). ClpX or ClpP detected by Western using α-ClpX or α-ClpP respectively (unfilled triangles) were used as loading control.

(A) CpdR expression levels using pRX2-M2 in *C. crescentus* Δ*cpdR* strain (related to Figure 5A).
(B) CpdR expression levels using pHX-M2 in *C. crescentus* wildtype strain (related to Figure 5B).
(C) CpdR expression levels using pHX-M2 in *C. crescentus* Δ*pdeA* strain (related to Figure 5C).
(D) CpdR expression levels using pHX-M2 in *C. crescentus* Δ*cpdR* Δ*cpdR* P_{xyl}-*clpX-gfp* strain (related to Figure 5D).
(E) CpdR expression levels using pHX-M2 in *C. crescentus* Δ*cpdR* strain (related to Figure 7E).

(A-E) performed in duplicates. Representative gels are shown.

Figure S6, related to Figure 6.

(A) Wildtype SspB and non-degradable variant SspB* show similar concentration-dependent adaptor activity. *In vitro* degradation of GFP-ssrA-SS (1μM) by ClpXP (0.2μM $ClpX_6$, 0.4μM $ClpP_{14}$) in the presence of increasing concentrations of SspB or the non-degradable SspB*.

(B) Non-degradable CpdRDD does not suppress substrate delivery, however CpdR wildtype can suppress substrate delivery due to competition for degradation with its own substrate. *In vitro* degradation of substrate GFP-PdeA (1μM) by ClpXP (0.2μM $ClpX_6$, 0.4μM $ClpP_{14}$) in the presence of increasing concentrations of CpdR WT/DD. (i and ii) show the activity from two independent purification of CpdRWT/DD proteins.

(C) Effect of SspB(SBD) on levels of GFP-ssrA-SS *in vivo* (related to Figure 6F). As described in Figure 6F, Flag-tagged GFP-ssrA-SS reporter (detected by Western α-GFP) was integrated in *C. crescentus* at the chromosomal *vanA* locus and expressed by addition of 1mM vanillate. SspB(substrate binding domain, SBD, residue 1-125) is expressed from a high-copy plasmid JS14 (repressible by 0.2% glucose and inducible by 0.2% xylose, detected by Western blotting with α-FLAG). Impact of FLAG-SspB(SBD) expression on FLAG-GFP-ssrA-SS levels is compared to a strain harboring JS14 (empty plasmid) and a Δ*sspB* strain harboring JS14 (empty plasmid).

(D) *In vitro* degradation profile of the non-degradable variant of CpdRH104A, CpdRH104ADD. (i) CpdR WT/H104A/H104ADD (10μM) degradation by ClpXP (0.4μM $ClpX_6$, 0.8μM $ClpP_{14}$) was evaluated. (ii) Adaptor activity of CpdRH104ADD was compared to CpdRH104A and CpdRDD. *In vitro* degradation performed using 1μM GFP-PdeA reporter substrate, 1mM GTP, 0.4μM $ClpX_6$, 0.8μM $ClpP_{14}$. CpdRH104ADD is more active than CpdRH104A, perhaps because CpdRH104A is also a degradation substrate for ClpXP.

(E) Effect of CpdRH104ADD on PdeA levels *in vivo* (related to Figure 6G). As described in Figure 6G, FLAG-tagged PdeA reporter is chromosomally integrated in *C. crescentus* for vanillate-induced expression, and FLAG-tagged CpdRH104ADD is expressed from the plasmid JS14 (both detected by Western blotting with α-FLAG). Impact of FLAG-CpdRH104ADD expression on FLAG-PdeA levels is compared to a strain harboring JS14 (empty plasmid) and a Δ*cpdR::tet* strain harboring JS14 (empty plasmid).

(A,B) performed in duplicates. (C,D) performed in triplicates. Representative gels are shown.

Figure S7, related to Figure 7.

(A) GFP-McpA degradation by ClpXP in the presence of CpdR H104A variant. GFP-McpA (1μM) degradation by ClpXP (0.2μM $ClpX_6$, 0.4μM $ClpP_{14}$) when mediated by CpdR WT or CpdRH104A variant (2.5μM).

(B) (i) McpA(cyto) degradation by ClpXP. Degradation of the isolated cytoplasmic domain of McpA (1μM) by ClpXP (0.2μM $ClpX_6$, 0.4μM $ClpP_{14}$) in the absence and presence of CpdR (2.5μM). **(ii) McpA(cyto) degradation in the FKBP/FRB tethering system.** Degradation profile of McpA(cyto) (1μM) by FKBP-ΔN-ClpXP mediated by FRB-CpdR (±rapamycin/FRB-CpdR/NTD_{ClpX} fragment).

(C) CtrA degradation in the FKBP/FRB tethering system. Degradationof CtrA (3μM) bound to cognate DNA (5μM FliF promoter) by FKBP-ΔN-ClpXP (±FRB-CpdR/NTD_{ClpX} fragment/additional adaptors (RcdA, PopA, cdG)) in the presence of rapamycin.

(D) GFP-CtrA RD+15 degradation in the FKBP/FRB tethering system. Degradation of GFP-tagged CtrA RD+15 (1μM) by FKBP-ΔN-ClpXP (±FRB-CpdR/NTD_{ClpX} fragment/additional adaptors (RcdA, PopA, cdG)/rapamycin). RD+15 omits the DNA-binding domain of CtrA, and contains the N-terminal receiver domain (RD) of CtrA critical for the multi-adaptor delivery and the C-terminus 15 residues that are important for recognition by ClpXP ATPase domain (Smith et al., 2014). Graphs are represented as mean ± SD, n=3. Tukey post hoc test built on one-way analysis of variance (ANOVA), performed using GraphPad Prism, indicate that tethered FRB-CpdR (i.e. plus rapamycin) in the presence of other adaptors (RcdA, PopA-cdG) and NTD_{ClpX} together result in a slightly higher rate of delivery compared to addition of only NTD_{ClpX} (***$p<0.001$) or the additional adaptors (RcdA and PopA in the presence of cdG) (**$p<0.01$).

(E) GFP-ssrA degradation is not enhanced in the FKBP/FRB tethering system. Degradation of GFP-ssrA (1μM) by FKBP-ΔN-ClpXP (±FRB-CpdR/NTD_{ClpX} fragment/additional adaptors (RcdA, PopA, cdG)) in the presence of rapamycin. Graphs are represented as mean ± SD, n=3.

Concentrations of proteins used in the above described FKBP/FRB tethering system are: 0.4μM FKBP-ΔN-$ClpX_6$, 0.8μM $ClpP_{14}$, 10μM rapamycin, 3μM FRB-CpdR, 25μM NTD_{ClpX}, 4μM RcdA, 1μM PopA, 20μM cdG.

(A-E) performed in triplicates. Representative gels are shown.

SUPPLEMENTAL EXPERIMENTAL PROCEDURES

Bacterial strains

E. coli Top 10 strain was used for cloning. BL21 DE3 strain was used for expression of recombinant protein under the control of isopropyl-beta-D-thiogalactopyranoside (IPTG)-inducible T7 promoter.

BACTH *E. coli cya clpX* strain (EPC452, F^-, *cya-99*, *araD139, galE15, galK16, rpsL1 (Str^r)*, *hsdR2, mcrA1, mcrB1,* Δ*clpX*) was constructed by P1 bacteriophage (gift from Professor Steven Sandler; UMass Amherst) transduction of a FRT-flanked Δ*clpX*::*kan* marker into the BACTH reporter strain BTH101 (Euromedex). After selection on LB plate containing 50μg/mL kanamycin, transduction of the ClpX knock-in genotype was verified by Western blot using affinity purified *E. coli* ClpX antibody. To remove the kanamycin marker, the *clpX* knock-in strain was transformed with pCP20 which expresses flippase to promote recombination between FRT sites flanking the kanamycin cassette. Removal of the kanamycin cassette allows for pKT25 (kan^R) to be utilized in BACTH interaction studies.

DNA cloning

BACTH plasmids

CpdR, PdeA and ClpX are cloned in frame into the XbaI and EcoRI site of the multiple cloning site of pKT25 or pUT18C downstream of the T25 and T18 gene fragment. Untagged ClpX, ClpX R367K, ClpX E184Q, and NTD_{ClpX} (residues 1-61) sequences were cloned into pCL1920 by Gibson assembly (Gibson et al., 2009) (pCL1920 Lac promoter DNA sequence (upper case) transitions into the ClpX N-terminus (lower case) as shown: TCACACAGGAAACAGCTatgacgaaagccgcgagcggcga). pCL1920 backbone was prepared by PCR for the Gibson reaction.

Plasmids expressed for *in vitro* protein purification

ClpXA is composed of ClpX residues 1-61 and ClpA residues 145-767. ClpX residues 1-61 fragment was obtained by PCR using pET23-ClpX (*C. crescentus* ortholog) as template. pET23 containing ClpA residues 145-767 was obtained by PCR using pET23-ClpA C-terminal Δ9 as template. These fragments were combined by Gibson assembly to create the plasmid for expressing untagged ClpXA in BL21 strain. The nine C-terminal residues of ClpA (residues 768-776) are omitted because it acts as an intrinsic auto-degradation tag *in vitro* as previously reported for its *E. coli* ortholog (Maglica et al., 2008). Removal of ClpA N-terminus (1-144) was determined through alignment between *C. crescentus* ClpA and *E. coli* ClpA, given previous domain studies of *E. coli* ClpA and sequence alignment reported in that work showing the conservation of the N-domain region between divergent organisms (Cranz-Mileva et al., 2008).

FKBP-ΔN-ClpX is constructed similar to a previous study (Davis et al., 2009), and consists of the following sequence from N to C-terminus: N-terminal human FKBP12 protein (108 residues), residues 139–165 of *E. coli* SspB, a His_6 tag, residues SSHM, residues 59–420 of *C. crescentus* ClpX. PCR of the "FKBP12-SspB(139-165)-His_6-SSHM" fragment was done using pACYC-FKBP-ΔN-ClpX (*E. coli* ortholog) (Davis et al., 2009) as template. Backbone fragment containing ΔN-ClpX (*C. crescentus* ortholog) was amplified using pET23-ΔN-ClpX (*C.*

crescentus ortholog). The two PCR fragments were combined by Gibson assembly to produce pET23- FKBP-ΔN-ClpX (*C. crescentus*).

SspB-FRB consists of the following sequence from N to C-terminus: *C. crescentus* SspB residues 10-125 that contains the ssrA binding domain (Chien et al., 2007a), $(GGSG)_2$ linker, and FRB. CpdR was N-terminally tagged with FRB with the $(GGSG)_2$ linker in between to allow for flexibility of the construct. Notably, FRB-CpdR was rapidly degraded by FKBP-ΔN-ClpX•ClpP in the presence of rapamycin. Replacing the CpdR C-terminal intrinsic degradation tag (FRB-CpdRDD) did not block degradation, but addition of MD_6 residues to the N-terminus of FRB-CpdRDD did, suggesting that the exposed FRB N-terminus is recognized for degradation by FKBP-ΔN-ClpX•ClpP/rapamycin. The FRB-CpdR reported throughout this paper refers to this MD_6-FRB-CpdRDD construct. Similarly, FRB-PdeA was constructed to contain an N-terminal MD_6-FRB so as to prevent N-terminal recognition by FKBP-ΔN-ClpX•ClpP/rapamycin. MD_6-FRB-PdeADD was constructed with replacement of the PdeA C-terminal intrinsic degradation tag. All these FRB fusion constructs were cloned into pET23-His-SUMO backbone by Gibson assembly.

CpdR variants (point mutations or C-terminus DD mutation) were generated by site-directed mutagenesis performed on pET23 His_6-SUMO-CpdR for protein expression.

NTD_{ClpX} fragment consist of residues 1-61 of *C. crescentus* ClpX was cloned into pET28-His-thrombin backbone.

GFP-ssrA-SS where the C-terminus Ala-Ala residue is mutated to Ser-Ser and cloned into ML375.

The cytosolic portion of McpA (residues 251-657) was amplified from *Caulobacter* genomic DNA, and cloned into pET23 His_6-SUMO with $mGFP_{mut3}$ on the N-terminus of the cytosolic McpA by restriction digestion-ligation. Similarly, the isolated cytosolic portion of McpA was also cloned into pET23 His_6-SUMO expression vector for production of the untagged version of McpA.

Plasmids for *in vivo* protein expression in *C. crescentus*

Site-directed mutagenesis was performed on pENTR-CpdR or pENTR-CpdR D51A. The pENTR-variants were then subcloned using the Gateway System (Invitrogen) into pHX-M2-DEST, pRX2-M2-DEST plasmids (Skerker, et. al. 2005; Thanbichler, et. al. 2007) or JS14-M2-DEST. These plasmids enable expression of M2-epitope tagged CpdR WT/variants.

M2-PdeA and M2-GFP-ssrA-SS were cloned into pVGFPC-2 (Thanbichler et al., 2007) at the NdeI and NheI sites. pVGFPC-2 is an integrating plasmid that chromosomally integrates into the *vanA* locus in *C. crescentus* to generate vanillate controllable induction.

Protein purification by affinity chromatography

Recombinant proteins were overexpressed from IPTG-inducible pET plasmids and purified as previously reported (Rood, et al, 2012; Bhat, et al. 2013). CpdR, PdeA, McpA (and their

variants) were expressed as C-terminal fusions to a his-tagged SUMO domain in BL21DE3 plysS cells. Purification of the fusions, cleavage of the SUMO domain, and separation of the cleaved protein were performed as before (Wang et al., 2007). CpdR and variants were further purified by size exclusion chromatography. SspB (and variants), CtrA (and GFP-CtrA RD+15), RcdA, and PopA are his-tagged proteins that were purified via standard Ni-NTA protocols (Qiagen). CckA-HK, CckA-RD, ChpT, GFP-PdeA are also his-tagged proteins that were purified via standard Ni-NTA protocols, followed by size exclusion chromatography. ClpX, ΔN-ClpX, ClpA, ClpXA, FKBP-ΔN-ClpX, and NTD_{ClpX} were purified first by Ni-NTA protocol and thrombin cleaved if his-tagged, followed additional column chromatography purifications (phenylsepharose, hydroxyapatite, MonoQ column or size exclusion chromatography) (Levchenko et al., 2000; Chien et al., 2007a). Detailed protocols are available upon request.

Bacterial adenylate cyclase two-hybrid (BACTH) assay (further details)

Interaction between two proteins of interest results in cAMP production, triggering the expression of several resident genes that allows catabolism of maltose or lactose. BACTH plasmid transformants were examined using two methods: (i) Evaluation of McConkey agar media containing maltose. Resuspended colonies were streaked on McConkey agar containing 1% maltose, 0.5mM IPTG, 50μg/mL kanamycin, 100μg/mL ampicillin. For Figure 4H, cells were grown to exponential phase before deposition as 2μL droplets of cells (diluted equally to OD600=0.3) on the McConkey agar. (ii) β-galactosidase activity. Cells from the McConkey plates were resuspended in Z-buffer (60mM Na2HPO4.7H2O, 40mM NaH2PO4.H2O, 10mM KCl, 1mM MgSO4.7H2O, 50mM β-mercaptoethanol) before lysis using 0.01% SDS and chloroform (100μL into 500μL samples), and measurement of the supernatant for β-galactosidase activity (Griffith and Wolf, 2002). We report the rates of formation of the yellow chromophore o-nitrophenol (ONP) as the hydrolytic product of the action of β-galactosidase on a colorless lactose analog, o-nitrophenyl-D-galactoside (ONPG), as assayed using a 96-well clear plate using a Spectramax M5 (Molecular Devices) microplate reader. Measurements of ONP were conducted at 30°C using absorbance at 420nm, and the rate of formation was normalized by the cell density (measured using OD600 before lysis of the cells).

Western blotting

Antibodies against CtrA (MA588), PdeA (MA590), ClpX (MA584), ClpP (MA586), CpdR (HM6663), Flag-M2 (Sigma F1804) and GFP (Clontech JL-8) were used in this study. Secondary antibodies used wre goat anti-rabbit IGG HRP (Millipore AP187P), goat anti-rabbit IRDye 800CW (Licor 926-32210), and goat anti-mouse IRDye 680LT (Licor 926-68021). Affinity purified α-PdeA was used throughout. Affinity purified α-ClpX and α-CpdR were used for BACTH plasmid expression detection.

Millipore Immobilon Western Chemiluminescent HRP substrate (ECL) was used to detect the HRP-conjugated secondary antibody for Figures 4, 5, 7, and S6A. During the course of this work, our lab had transitioned from using ECL to using an infrared imager. Western blots shown in Figure 3, 6, S1, S3, S5, and S6B-E were imaged using IRDye secondary antibodies and a Licor Odyssey CLx infrared imager. Also, note that in Figure 7E, CtrA was detected using α-CtrA (rabbit) first, before detection using α-ClpP (rabbit) where detection of both CtrA and ClpP

can be seen. Cross-reactivity between α-CtrA and α-ClpP is minimal, so the co-immunoblots are shown. For Figure S6B-E, α-Flag (mouse) was detected first, followed by α-ClpP (rabbit). The images are the co-immunoblots detected by infrared imager where the signal detected from the different channels (680 and 800) are overlaid.

CpdR Phyre modeling and sequence alignment

To build a 3D homology model of CpdR, the online protein fold recognition server Phyre 2 (Kelley and Sternberg, 2009) was used. Conserved residues amongst α-proteobacteria CpdR orthologs were determined as previously, selecting only one species for each genus (Brilli et al., 2010).

Radioactive phosphotransfer profiling

Radiolabeled phosphorylation of CpdR using cognate phosphorelay proteins (Figure S4A) were performed in H-Buffer, with additional 5mM $MgCl_2$ to ensure sufficiency for the phosphorylation reaction to occur. A premix of 0.167 μCi/μL of radiolabeled ATP (γ^{32}P, Perkin Elmer) and 500μM ATP were added to CckA (split version (Chen et al., 2009)) for an incubation period of 40 minutes at 30°C to allow for autophosphosphorylation of the histidine kinase. The phosphotransfer profiling was initiated upon addition of 1.25μM of the phosphotransferase ChpT and 5μM of CpdR and its variants. Reaction samples at 30°C were taken after 5 minutes, quenched with SDS loading dye, and frozen immediately. Samples were examined by SDS-PAGE, followed by phosphorimaging.

Bacterial strains used in this work

Strain	Description	Reference
TOP10	*E. coli* cloning strain.	Invitrogen
BL21(DE3)pLysS	*E. coli* strain for recombinant protein expression strain	Invitrogen
BTH101	*E. coli* BACTH reporter strain lacking functional cya (adenylate cyclase gene for expressing cAMP)	(Karimova et al., 1998); Euromedex
BTH101 Δ*clpX*	*E. coli* BTH101 with markerless deletion of *clpX* using Flp-FRT recombination	This study
BPC129	*E. coli* W3110 ΔclpX::kan	T. Baker (MIT)
NA1000 (CB15N)	Synchronizable strain of *C. crescentus*	(Evinger and Agabian, 1977)
NA1000 Δ*pdeA*	NA1000 with markerless in frame deletion of pdeA	(Abel et al., 2011)
NA1000 Δ*cpdR::tetR*	Disruption of the *cpdR* gene by a Tet^R cassette (Tet^R)	(Skerker et al., 2005)
NA1000 Δ*cpdR::tetR, xylX::*P_{xylX}-*clpX-gfp*	NA1000 Δ*cpdR::tetR* ϕCr30 transduced with xylose-inducible *clpX-gfp* from 000 *xylX::*P_{xylX}-*clpX-gfp* (Iniesta et al., 2006) (Tet^R Kan^R)	This study
NA1000 Δ*sspB*	NA1000 with markerless deletion of *sspB*	Lessner, et al. 2007
W3110	*E. coli* wildtype strain	T. Baker (MIT)
W3110 Δ*clpX*	Kanamycin marker was removed from *E. coli* W3110 ΔclpX::kan by flip-FRT	T. Baker (MIT)
NA1000 *vanA::*P_{vanA}-M2-PdeA + JS14	NA1000 with chromosomally integrated vanillate-inducible M2-PdeA, and high copy empty plasmid JS14 (Kan^R $Chlor^R$)	This study
NA1000 *vanA::*P_{vanA}-M2-PdeA + JS14-M2-P_{xyl}-CpdRH104ADD	NA1000 with chromosomally integrated vanillate-inducible M2-PdeA, and high copy plasmid JS14 expressing M2-tagged CpdRH104ADD (Kan^R $Chlor^R$)	This study
NA1000 *vanA::*P_{vanA} -M2-PdeA Δ*cpdR::tetR* +JS14	NA1000 with chromosomally integrated vanillate-inducible M2-PdeA ϕCr30 transduced with NA1000 Δ*cpdR::tetR,* and	This study

	high copy empty plasmid JS14 (Tet^R Kan^R $Chlor^R$)	
NA1000 *vanA::*P_{vanA} -M2-GFP-ssrA-SS	NA1000 with chromosomally integrated vanillate-inducible M2-GFP-ssrA-SS (Kan^R)	This study
NA1000 *vanA::*P_{vanA} -M2-GFP-ssrA-SS+ JS14-P_{xyl}-M2-SspB(SBD)	NA1000 with chromosomally integrated vanillate-inducible M2-GFP-ssrA-SS, and high copy plasmid JS14 expressing M2-tagged SspB(SBD) (Kan^R $Chlor^R$)	This study
NA1000 *vanA::*P_{vanA} -M2-GFP-ssrA-SS Δ*sspB* +JS14	NA1000 Δ*sspB* ϕCr30 transduced with NA1000 *vanA::*P_{vanA} -M2-GFP-ssrA-SS, and high copy empty plasmid JS14 (Tet^R Kan^R $Chlor^R$)	This study
NA1000 Δ*cpdR::tetR* + pRX-M2-CpdR	NA1000 Δ*cpdR::tetR* and low copy plasmid with xylose-inducible expression of M2-CpdR (Tet^R Kan^R)	This study
NA1000 Δ*cpdR::tetR* + pRX-M2-CpdRR106A	NA1000 Δ*cpdR::tetR* and low copy plasmid with xylose-inducible expression of M2-CpdRR106A (Tet^R Kan^R)	This study
NA1000 Δ*cpdR::tetR* + pRX-M2-CpdRH104A	NA1000 Δ*cpdR::tetR* and low copy plasmid with xylose-inducible expression of M2-CpdRH104A (Tet^R Kan^R)	This study
NA1000 Δ*cpdR::tetR* + pHX-M2-CpdR	NA1000 Δ*cpdR::tetR* and medium copy plasmid with xylose-inducible expression of M2-CpdR (Tet^R $Spec^R$)	This study
NA1000 Δ*cpdR::tetR* + pHX-M2-CpdRR106A	NA1000 Δ*cpdR::tetR* and medium copy plasmid with xylose-inducible expression of M2-CpdRR106A (Tet^R $Spec^R$)	This study
NA1000 Δ*cpdR::tetR* + pHX-M2-CpdRH104A	NA1000 Δ*cpdR::tetR* and medium copy plasmid with xylose-inducible expression of M2-CpdRH104A (Tet^R $Spec^R$)	This study
NA1000 + pHX-M2-CpdRD51A	NA1000 and medium copy plasmid with xylose-inducible expression of M2-CpdRD51A ($Spec^R$)	This study
NA1000 + pHX-M2-CpdRD51A R106A	NA1000 and medium copy plasmid with xylose-inducible expression of M2-CpdRD51A R106A ($Spec^R$)	This study
NA1000 + pHX-M2-CpdRD51A H104A	NA1000 and medium copy plasmid with xylose-inducible expression of M2-CpdRD51A H104A ($Spec^R$)	This study
NA1000 Δ*pdeA* + pHX-M2-CpdRD51A	NA1000 Δ*pdeA* and medium copy plasmid with xylose-inducible expression of M2-CpdRD51A ($Spec^R$)	This study
NA1000 Δ*pdeA* + pHX-M2-CpdRD51A R106A	NA1000 Δ*pdeA* and medium copy plasmid with xylose-inducible expression of M2-CpdRD51A R106A ($Spec^R$)	This study
NA1000 Δ*pdeA* + pHX-M2-CpdRD51A H104A	NA1000 Δ*pdeA* and medium copy plasmid with xylose-inducible expression of M2-CpdRD51A H104A ($Spec^R$)	This study
NA1000 Δ*cpdR::tetR xylX::*P_{xylX}-*clpX-gfp* + pHX-M2-CpdR	NA1000 Δ*cpdR::tetR* and medium copy plasmid with xylose-inducible expression of M2-CpdR (Tet^R Kan^R $Spec^R$)	This study
NA1000 Δ*cpdR::tetR xylX::*P_{xylX}-*clpX-gfp* + pHX-M2-CpdRR106A	NA1000 Δ*cpdR::tetR* and medium copy plasmid with xylose-inducible expression of M2-CpdRR106A (Tet^R Kan^R $Spec^R$)	This study
NA1000 Δ*cpdR::tetR xylX::*P_{xylX}-*clpX-gfp* + pHX-M2-CpdRH104A	NA1000 Δ*cpdR::tetR* and medium copy plasmid with xylose-inducible expression of M2-CpdRH104A (Tet^R Kan^R $Spec^R$)	This study

Plasmids used in this work

Plasmid name	**Description**	**Reference**
pET23 His_6-SUMO	T7 promoter; for His_6SUMO fusion protein expression (Amp^R)	(Wang et al., 2007)
pET23b	T7 promoter; for protein expression (Amp^R)	Novagen
ML375 DEST (375)	DEST expression plasmid; T7 promoter; for His_6 thrombin fusion protein expression (Amp^R)	(Skerker et al., 2005)
pET28b His_6-thrombin	DEST expression plasmid; T7 promoter; for His_6 thrombin fusion protein expression (Kan^R)	Novagen
pCP20	Temperature-sensitive origin of replication, confers ampicillin resistance, and encodes the flippase (FLP) recombinase (Amp^R)	(Cherepanov and Wackernagel, 1995)
pET23 His_6-SUMO CpdR	For purification of full length CpdR (Amp^R)	(Abel et al., 2011)
pET23 His_6SUMO CpdRD51A	For purification of CpdRD51A (Amp^R)	(Abel et al., 2011)
pET23 His_6SUMO CpdRDD	For purification of CpdRDD (Amp^R)	This study
pET23 His_6SUMO CpdRR106A	For purification of CpdRR106A (Amp^R)	This study
pET23 His_6SUMO CpdRH104A	For purification of CpdRH104A (Amp^R)	This study
pET23 His_6SUMO CpdRH104ADD	For purification of CpdRH104ADD (Amp^R)	This study

pET23 His_6SUMO MD_6-FRB-CpdRDD	For purification of MD_6-FRB-tagged CpdRDD (Amp^R)	This study
pET23 His_6SUMO PdeA	For purification of full length PdeA (Amp^R)	(Abel et al., 2011)
pET23 His_6SUMO PdeA-ssrA	For purification of PdeA-ssrA (Amp^R)	This study
375 His_6-GFP PdeA	For purification of N-terminally his-tagged GFP fused to the N-terminus of PdeA (Amp^R)	(Rood et al., 2012)
pET23 His_6SUMO MD_6-FRB-PdeA	For purification of MD_6-FRB-tagged PdeA (Amp^R)	This study
pET23 His_6SUMO MD_6-FRB-PdeADD	For purification of MD_6-FRB-tagged PdeADD (Amp^R)	This study
pET23 *C. crescentus* ClpX	For purification of untagged *C. crescentus* ClpX (Amp^R)	(Rood et al., 2012)
pET28 His_6thrombin *C. crescentus* ClpX	For purification of His-thrombin *C. crescentus* ClpX (Kan^R)	(Chien et al., 2007a)
pET23 ΔN-ClpX (*C. crescentus* ortholog)	For purification of untagged *C. crescentus* ΔN-ClpX (Amp^R)	(Bhat et al., 2013)
pET23 *C. crescentus* ClpAΔC9	For purification of untagged ClpA without last 9 C-terminal residues to prevent auto-degradation (Amp^R)	(Williams et al., 2014)
pET23 *C. crescentus* ClpXA	For purification of untagged NTD_{ClpX} (1-61) fused to ClpA (145-767) [ΔNTD_{ClpA} and ΔC-terminal 9 residues]	This study
pET28 His_6 *C. crescentus* NTD_{ClpX}	For purification of untagged NTD_{ClpX} (1-61) through thrombin cleavage (Kan^R)	This study
pET23 FKBP-His_6- *C. crescentus* ClpXΔN	For purification of FKBP-linker fused to ClpXΔN (Amp^R)	This study
pET14b His_6-*E. coli* ClpX	For purification of His-tagged *E. coli* ClpX (Amp^R)	(Levchenko et al., 1997)
pQE70 *C. crescentus* $ClpPHis_6$	Lac inducible plasmid for purification of his-tagged *C. crescentus* ClpP (Amp^R)	(Chien et al., 2007a)
pQE70 *E. coli* $ClpPHis_6$	For purification of His-tagged *E. coli* ClpP (Amp^R)	(Kim et al., 2000)
375 His_6GFP- *C. crescentus* ssrA-SS	For purification of GFP-ssrA-ss where C-terminal Ala-Ala are mutated to Ser-Ser (Amp^R)	This study
pBAD GFP- *C. crescentus* ssrA	For purification of GFP-ssrA (Amp^R)	(Chien et al., 2007a)
pET28 His_6 CC SspB	For purification of the *C. crescentus* ortholog of the degradable SspB wildtype (residues 1-162) (Kan^R)	(Chien et al., 2007a)
pET28 His_6 *C. crescentus* SspB N-terminal Δ9	For purification of the *C. crescentus* ortholog of the nondegradable SspB variant (residues 10-162), SspB* (Kan^R)	(Chien et al., 2007a)
pET28 His_6 *C. crescentus* SspB(substrate binding domain, SBD)	For purification of the *C. crescentus* ortholog of the SspB variant (residues 10-125), SspB(SBD) (Kan^R)	(Chien et al., 2007b)
pET23 His_6SUMO *C. crescentus* SspB-FRB	For purification of SspB(10-125, SBD)-FRB (Amp^R)	This study
pHis$_6$-MBP-CckA-HK	For purification of His_6-MBP-CckA-HK (Amp^R)	(Chen et al., 2009)
pTRX-His_6CckA-RD	For purification of His_6-TRX-CckA-RD (Amp^R)	(Chen et al., 2009)
pTRX-His_6ChpT	For purification of His_6-TRX-ChpT (Amp^R)	(Biondi et al., 2006)
pET23 His_6SUMO GFP_{mut3}-cytoplasmic McpA	For purification of GFPmut3-McpA residues 251-657 (Amp^R)	This study
pET23 His_6SUMO cytoplasmic McpA	For purification of McpA residues 251-657 (Amp^R)	This study
pET28 His_6CtrA	For purification of His_6-CtrA (Amp^R)	(Chien et al., 2007a)
pET28 His_6GFP-CtrA RD+15	For purification of His_6-GFP-CtrA-RD+15 (Amp^R)	(Smith et al., 2014)
pET28 His_6RcdA	For purification of His_6-RcdA (Amp^R)	(Chien et al., 2007a)
pET28 His_6PopA	For purification of His_6-PopA (Amp^R)	(Smith et al., 2014)
pKT25	Derivative of pACYC184 that encodes the T25 fragment of CyaA (amino acids 1–224) driven by wildtype P_{lac} (Kan^R)	(Karimova et al., 1998); Euromedex
pUT18C	Derivative of pBluescript II KS, compatible with pKT25, that encodes the T18 fragment of CyaA (amino acids 225–399) driven by wildtype P_{lac} (Amp^R)	(Karimova et al., 1998); Euromedex
pUT18C- *C. crescentus* ClpX	*E. coli* plasmid for expressing T18-ClpX using P_{lac} (Amp^R)	This study, similar to (Abel et al., 2011)
pUT18C-PdeA	*E. coli* plasmid for expressing T18-PdeA using P_{lac} (Amp^R)	This study, similar to (Abel et al., 2011)
pKT25-PdeA	*E. coli* plasmid for expressing T25-PdeA using P_{lac} (Kan^R)	This study, similar to

		(Abel et al., 2011)
pKT25-CpdR	*E. coli* plasmid for expressing T25-CpdR using P_{lac} (Kan^R)	This study, similar to (Abel et al., 2011)
pKT25-CpdRR106A	*E. coli* plasmid for expressing T25-CpdRR106A using P_{lac} (Kan^R)	This study
pKT25-CpdRH104A	*E. coli* plasmid for expressing T25-CpdRH104A using P_{lac} (Kan^R)	This study
pCL1920	Low copy expression plasmid for expression in *E. coli,* compatible for co-expression with BACTH plasmids, wildtype P_{lac} ($Spec^R$)	(Lerner and Inouye, 1990)
pCL1920-*C. crescentus* ClpX	Plasmid for expressing ClpX (*C. crescentus* ortholog) using P_{lac} in *E. coli* ($Spec^R$)	This study
pCL1920- *C. crescentus* ClpXR367K	Plasmid for expressing ClpXR367K (*C. crescentus* ortholog) using P_{lac} in *E. coli* ($Spec^R$)	This study
pCL1920- *C. crescentus* ClpXE184Q	Plasmid for expressing ClpXE184Q (*C. crescentus* ortholog) using P_{lac} in *E. coli* ($Spec^R$)	This study
pCL1920- *C. crescentus* NTD_{ClpX}	Plasmid for expressing NTD_{ClpX} (*C. crescentus* ortholog) using P_{lac} in *E. coli* ($Spec^R$)	This study
pRX2 M2-DEST	Low copy DEST vector; xylose promoter; for expression of FLAG-M2 tagged constructs (Kan^R) in *C. crescentus*	Derived from (Thanbichler et al., 2007)
pRX2-M2-CpdR WT	Plasmid for low copy expression of Flag-M2-tagged CpdR WT in *C. crescentus* (Kan^R)	This study
pRX2-M2-CpdRR106A	Plasmid for low copy expression of Flag-M2-tagged CpdRR106A in *C. crescentus* (Kan^R)	This study
pRX2-M2CpdRH104A	Plasmid for low copy expression of Flag-M2-tagged CpdRH104A in *C. crescentus* (Kan^R)	This study
pRX2-M2-GFP	Plasmid for low copy expression of Flag-M2-tagged GFP in *C. crescentus* (Kan^R)	This study
pHMX M2-DEST	Medium copy DEST vector; xylose promoter; for expression of FLAG-M2 tagged constructs ($Spec^R$)	(Skerker et al., 2005)
pHMX-CpdR WT	Plasmid for medium copy expression of Flag-M2-tagged CpdR WT in *C. crescentus* ($Spec^R$)	This study
pHMX-CpdRR106A	Plasmid for medium copy expression of Flag-M2-tagged CpdRR106A in *C. crescentus* ($Spec^R$)	This study
pHMX-CpdRH104A	Plasmid for medium copy expression of Flag-M2-tagged CpdRH104A in *C. crescentus* ($Spec^R$)	This study
pHMX-CpdRD51A	Plasmid for medium copy expression of Flag-M2-tagged CpdRD51A in *C. crescentus* ($Spec^R$)	This study
pHMX-CpdRD51A R106A	Plasmid for medium copy expression of Flag-M2-tagged CpdRD51A R106A in *C. crescentus* ($Spec^R$)	This study
pHMX-CpdRD51A H104A	Plasmid for medium copy expression of Flag-M2-tagged CpdRD51A H104A in *C. crescentus* ($Spec^R$)	This study
pHMX-GFP-AA	Plasmid for medium copy expression of Flag-M2-tagged GFP-AA in *C. crescentus* ($Spec^R$)	This study
pVan-M2-GFP-ssrA-SS	Plasmid for integration of Flag-M2-tagged GFP-ssrA-SS at the vanillate-modulatable promoter locus in *C. crescentus* (Kan^R)	This study
pVan-M2-PdeA	Plasmid for integration of Flag-M2-tagged PdeA at the vanillate-modulatable promoter locus in *C. crescentus* (Kan^R)	This study
JS14-Pxyl M2-DEST	Medium copy DEST vector; xylose promoter; for expression of FLAG-M2 tagged constructs ($Chlor^R$)	M. Laub (MIT)
JS14 (empty plasmid)	Empty medium copy plasmid for *C. crescentus* ($Chlor^R$)	M. Laub (MIT)
JS14- Pxyl M2-SspB(SBD)	Plasmid for medium copy expression of Flag-M2-tagged SspB (12-125, SBD) in *C. crescentus* ($Chlor^R$)	This study
JS14- Pxyl M2-CpdRH104ADD	Plasmid for medium copy expression of Flag-M2-tagged CpdRH104ADD in *C. crescentus* ($Chlor^R$)	This study

SUPPLEMENTAL REFERENCES

Abel, S., Chien, P., Wassmann, P., Schirmer, T., Kaever, V., Laub, M.T., Baker, T.A., and Jenal, U. (2011). Regulatory Cohesion of Cell Cycle and Cell Differentiation through Interlinked Phosphorylation and Second Messenger Networks. Mol. Cell *43*, 550–560.

Bhat, N.H., Vass, R.H., Stoddard, P.R., Shin, D.K., and Chien, P. (2013). Identification of ClpP substrates in *Caulobacter crescentus* reveals a role for regulated proteolysis in bacterial development. Mol. Microbiol. *88*, 1083–1092.

Biondi, E.G., Reisinger, S.J., Skerker, J.M., Arif, M., Perchuk, B.S., Ryan, K.R., and Laub, M.T. (2006). Regulation of the bacterial cell cycle by an integrated genetic circuit. Nature *444*, 899–904.

Brilli, M., Fondi, M., Fani, R., Mengoni, A., Ferri, L., Bazzicalupo, M., and Biondi, E.G. (2010). The diversity and evolution of cell cycle regulation in alpha-proteobacteria: a comparative genomic analysis. BMC Syst. Biol. *4*, 1–16.

Chen, Y.E., Tsokos, C.G., Biondi, E.G., Perchuk, B.S., and Laub, M.T. (2009). Dynamics of Two Phosphorelays Controlling Cell Cycle Progression in *Caulobacter cresccentus*. J. Bacteriol. *191*, 7417–7429.

Cherepanov, P.P., and Wackernagel, W. (1995). Gene disruption in *Escherichia coli*: TcR and KmR cassettes with the option of Flp-catalyzed excision of the antibiotic-resistance determinant. Gene *158*, 9–14.

Chien, P., Perchuk, B.S., Laub, M.T., Sauer, R.T., and Baker, T.A. (2007a). Direct and adaptor-mediated substrate recognition by an essential AAA+ protease. Proc. Natl. Acad. Sci. U. S. A. *104*, 6590–6595.

Chien, P., Grant, R. a, Sauer, R.T., and Baker, T. a (2007b). Structure and substrate specificity of an SspB ortholog: design implications for AAA+ adaptors. Structure *15*, 1296–1305.

Cranz-Mileva, S., Imkamp, F., Kolygo, K., Maglica, Ž., Kress, W., and Weber-Ban, E. (2008). The Flexible Attachment of the N-Domains to the ClpA Ring Body Allows their Use On Demand. J. Mol. Biol. *378*, 412–424.

Davis, J.H., Baker, T.A., and Sauer, R.T. (2009). Engineering Synthetic Adaptors and Substrates for Controlled ClpXP Degradation. J. Biol. Chem. *284*, 21848–21855.

Evinger, M., and Agabian, N. (1977). Envelope-Associated Nucleoid from *Caulobacter crescentus* Stalked and Swarmer Cells. J. Bacteriol. 294–301.

Gibson, D.G., Young, L., Chuang, R.-Y., Venter, J.C., Hutchison, C. a, and Smith, H.O. (2009). Enzymatic assembly of DNA molecules up to several hundred kilobases. Nat. Methods *6*, 343–345.

Hersch, G.L., Burton, R.E., Bolon, D.N., Baker, T.A., and Sauer, R.T. (2005). Asymmetric Interactions of ATP with the AAA+ ClpX6 Unfoldase: Allosteric Control of a Protein Machine. Cell *121*, 1017–1027.

Iniesta, A.A., McGrath, P.T., Reisenauer, A., McAdams, H.H., and Shapiro, L. (2006). A phospho-signaling pathway controls the localization and activity of a protease complex critical for bacterial cell cycle progression. Proc. Natl. Acad. Sci. U. S. A. *103*, 10935–10940.

Joshi, S.A., Hersch, G.L., Baker, T.A., and Sauer, R.T. (2004). Communication between ClpX and ClpP during substrate processing and degradation. Nat. Struct. Mol. Biol. *11*, 404–411.

Karimova, G., Pidoux, J., Ullmann, A., and Ladant, D. (1998). A bacterial two-hybrid system based on a reconstituted signal transduction pathway. Proc. Natl. Acad. Sci. U. S. A. *95*, 5752–5756.

Kelley, L.A., and Sternberg, M.J.E. (2009). Protein structure prediction on the Web: a case study using the Phyre server. Nat. Protoc. *4*, 363–371.

Kim, Y., Burton, R.E., Burton, B.M., Sauer, R.T., and Baker, T.A. (2000). Dynamics of Substrate Denaturation and Translocation by the ClpXP Degradation Machine. Mol. Cell *5*, 639–648.

Lerner, C.G., and Inouye, M. (1990). Low copy number plasmids for regulated low-level expression of cloned genes in Escherichia coli with blue/white insert screening capability. Nucleic Acids Res. *18*, 4631.

Levchenko, I., Yamauchi, M., and Baker, T.A. (1997). ClpX and MuB interact with overlapping regions of Mu transposase: implications for control of the transposition pathway. Genes Dev. *11*, 1561–1572.

Levchenko, I., Seidel, M., Sauer, R.T., and Baker, T.A. (2000). A Specificity-Enhancing Factor for the ClpXP Degradation Machine. Science *289*, 2354–2356.

Maglica, Z., Striebel, F., and Weber-Ban, E. (2008). An intrinsic degradation tag on the ClpA C-terminus regulates the balance of ClpAP complexes with different substrate specificity. J. Mol. Biol. *384*, 503–511.

Rood, K.L., Clark, N.E., Stoddard, P.R., Garman, S.C., and Chien, P. (2012). Adaptor-Dependent Degradation of a Cell-Cycle Regulator Uses a Unique Substrate Architecture. Structure *20*, 1–10.

Skerker, J.M., Prasol, M.S., Perchuk, B.S., Biondi, E.G., and Laub, M.T. (2005). Two-Component Signal Transduction Pathways Regulating Growth and Cell Cycle Progression in a Bacterium: A System-Level Analysis. PLoS Biol. *3*, 1770–1788.

Smith, S.C., Joshi, K.K., Zik, J.J., Trinh, K., Kamajaya, A., Chien, P., and Ryan, K.R. (2014). Cell cycle-dependent adaptor complex for ClpXP-mediated proteolysis directly integrates phosphorylation and second messenger signals. Proc. Natl. Acad. Sci. *111*, 14229–14234.

Thanbichler, M., Iniesta, A. a, and Shapiro, L. (2007). A comprehensive set of plasmids for vanillate- and xylose-inducible gene expression in *Caulobacter crescentus*. Nucleic Acids Res. *35*, 1–16.

Wang, K.H., Sauer, R.T., and Baker, T.A. (2007). ClpS modulates but is not essential for bacterial N-end rule degradation. Genes Dev. *21*, 403–408.

Williams, B., Bhat, N., Chien, P., and Shapiro, L. (2014). ClpXP and ClpAP proteolytic activity on divisome substrates is differentially regulated following the Caulobacter asymmetric cell division. Mol. Microbiol. *93*, 853–866.